(Received 19 October 2025, Accepted 3 December 2025, Scheduled 15 December 2025)

Shorted Microstrip Line Fed Wideband Design of E-Shape Microstrip Antenna Loaded with Printed Rectangular Resonator

Venkata A. P. Chavali[1] and Amit A. Deshmukh[2,*]

[1]Department of ECE, IIIT Surat, Surat, India
[2]Department of EXTC, SVKM's DJSCE, Mumbai, India

ABSTRACT: The shorted microstrip line fed design of an E-shape microstrip antenna loaded with a printed rectangular loop resonator is presented for wideband response on a thinner substrate. Wideband response is attributed to the optimum inter-spacing between the $TM_{1/2,0}$ resonant mode of shorted microstrip line feed, with respect to TM_{10} and modified TM_{02} modes on rectangular patch and TM_{20} mode on the printed rectangular loop. The design on a substrate of thickness $0.046\lambda_g$ achieves bandwidth of 227 MHz (23.56%) with a peak broadside gain of 7.1 dBi. The selection of microstrip line feed achieves wideband response on thinner substrate and harmonic rejection to the higher band frequencies. A methodology to design similar antennas as per specific wireless application is presented that yields similar result. An experimental verification has been carried out in the proposed design, which shows close agreement with the simulation.

1. INTRODUCTION

Microstrip antenna (MSA) finds wide applications in wireless communication, attributed to its low profile and planar configuration [1–3]. It was previously believed that MSAs were narrow bandwidth (BW) designs; however, numerous methods have been devised in recent decades to attain a wider BW. The simplest method of all is the use of a thicker substrate in combination with capacitive proximity feeding [4]. This method is very useful for antenna designs having the substrate of thickness greater than $0.08\lambda_g$. Multi-resonator gap-coupling method is another widely considered design, in which parasitic resonators slightly different in frequency are coupled to the fed patch [5–8]. The BW and gain in MSAs are increased by employing patches in the planar and stacked layers, while a cavity-backed configuration is considered [9, 10]. The multi-resonator configuration is simpler in design and fabrication, but it increases the antenna volume. A gap-coupled design of the shorted microstrip line feed with a regular shape MSA is reported that offers BW improvement with a marginal increment in the antenna size [11, 12]. But in the reported papers, details for designing a shorted microstrip line feed are not discussed. A modified shape of the radiating patch is also used to increase the MSA BW [13, 14]. While maintaining the single patch design, MSA BW is increased by employing a resonant slot [15–19]. While the suitable modifications in the ground plane are considered, wideband response using conventional or slot cut MSAs has been realized [20–24]. Slot cut MSA and modified ground plane designs are optimum methods since they provide single patch solution. But in these designs, either the antenna thickness is large ($> 0.06\lambda_g$) or back-lobe radiation reduces the antenna gain. In addition, these methods do not provide harmonic frequency rejection for the input radio frequency (RF) signal.

In this paper, the design of a shorted microstrip line fed E-shape MSA loaded with a printed resonant rectangular loop is proposed. The use of shorted microstrip line feeding helps in achieving a wideband response on lower substrate thickness and provides a harmonic frequency rejection using an E-shape patch. The use of a printed rectangular loop achieves a BW increment without the addition of parasitic resonator around the E-shape MSA. The limits of wideband response in E-shape MSA on thinner substrate are explained at the outset of this work. Shorted microstrip line feed design is used to provide a wider BW on a thinner substrate. On the overall substrate thickness of $0.046\lambda_g$ and adapting a three-layer air suspended configuration employing glass epoxy substrate ($\varepsilon_r = 4.3$, $h = 0.16$ cm), first the design of a rectangular microstrip antenna (RMSA) fed using a shorted microstrip line is studied. The antenna yields reflection coefficient $(S_{11}) \leq -10$ dB BW of 173 MHz (18.47%) with a peak broadside antenna gain of 7.2 dBi. A raise in the BW is achieved by loading the MSA with two parallel rectangular slots on the edge of the patch, resulting in an E-shape MSA. This design for the same substrate thickness achieves S_{11} BW of 198 MHz (20.93%). Further increment in the BW is obtained by loading the E-shape patch with a printed rectangular resonator loop. The resonator is added below the patch on the other side of substrate, thereby maintaining the same E-shape patch size. This gap-coupled E-shape MSA excited using shorted microstrip line feed achieves S_{11}

* Corresponding author: Amit A. Deshmukh (amitdeshmukh76@yahoo.com).

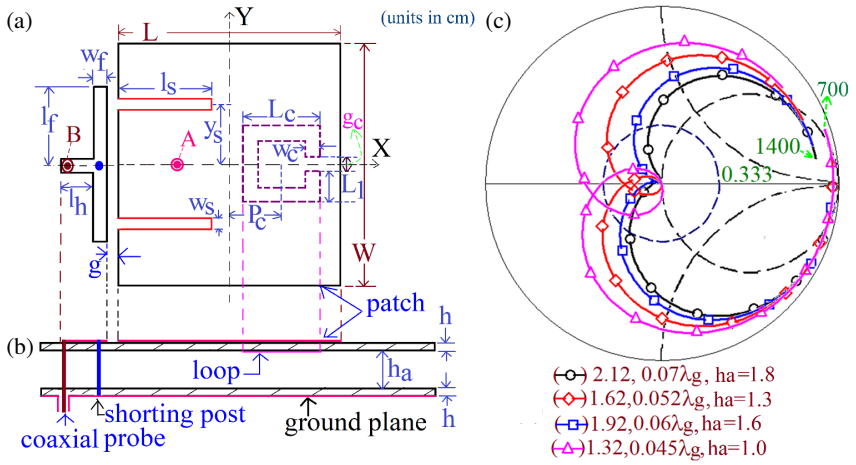

FIGURE 1. (a) (b) Shorted microstrip line fed E-shape MSA loaded with printed rectangular resonator, (c) smith chart for decreasing substrate thickness for E-shape MSA, (antenna dimensions in cm).

BW of 227 MHz (23.56%) with broadside peak gain of 7.1 dBi. Throughout the S_{11} BW, the antenna exhibits broadside radiation pattern. Thus, the proposed gap-coupled E-shape MSA attains S_{11} BW of nearly 24% on a thinner substrate ($0.046\lambda_g$), offering a maximum gain of more than 7 dBi. In addition, it provides rejection to harmonic frequencies of higher order modes in the E-shape patch. Considering all these design features together, the proposed design offers improved and optimum result. Thus, the technological innovation in this study is a design of a wideband E-shape MSA with a thinner substrate that offers harmonic rejection. A thorough tabular comparison analysis is covered later in the text to emphasize this. Finally, a formula for the resonant length at different patch modes in the optimal design is offered, along with a following process to create a comparable configuration around the particular frequency band that yields the same result. MSAs proposed in this paper are first simulated using CST software [26], followed by the experimental verifications, which shows a close agreement.

2. SHORTED MICROSTRIP LINE FED E-SHAPE MSA

The design of a shorted microstrip line fed E-shape MSA loaded with a printed rectangular loop resonator placed below the patch and on other side of the substrate is displayed in Figs. 1(a), (b). A three-layer air suspended structure is taken into consideration, with two FR4 layers separated by an air gap that is h_a cm in thickness. Initially the parametric variation is carried out to study the impedance response of coaxially fed E-shape MSA with dimensions $L = 12$, $W = 14$, $l_s = 6.6$, $y_s = 1.95$, $w_s = 0.5$ cm, against decreasing substrate thickness. The E-shape MSA offers optimum BW with a formation of loop within VSWR $= 2$ circle for $h_a = 1.8$ cm. The optimization procedure for E-shape patch is not described here as it is available in detail in the literature [25]. As seen in Fig. 1(c), the loop produced with the coaxial feed at point 'A' is not optimal inside the VSWR $= 2$ circle, when h_a decreases. This shifting in loop position is attributed to the increase in capacitive impedance offered by the pair of slots in E-shape MSA [25]. Thus, wideband response cannot be achieved in coaxial fed MSA on a thinner substrate.

To achieve the it, position of the feed needs to be shifted from the patch. A proximity feed, a method of non-contact feeding, can be employed. However, this also limits the BW on a thinner substrate. Another option is aperture coupling, but it is complex to design. Hence, the design of a shorted microstrip line feeding the MSA is considered. In this, the coaxial feed is present on the shorted microstrip line, as mentioned in Figs. 1(a), (b), i.e., at point 'B'. To assess the effects of shorted microstrip line exciting the patch, parametric variations are carried out using RMSA first, and Figs. 2(a)–(f) show the resonance frequency plots, Smith chart, and peripheral current distributions for it. As noted from Fig. 2(d), surface currents on shorted microstrip line feed shows one half wavelength variation over its vertical length, or quarter wavelength variation over half of the length. With this, the resonant mode is referred to as $\mathrm{TM}_{1/2,0}$ [30]. The first index refers to the variation along shorted length, which is the larger dimension of the feed line. As the variation is quarter wavelength in nature, modal index $\frac{1}{2}$ is considered. The second index is for variation along the orthogonal dimension in shorted microstrip line. As line width is very small, this variation is absent, and thus the corresponding modal index is 0.

At TM_{10} mode in RMSA, currents show half wavelength variation as given in Fig. 2(e). The increase in shorted length l_f reduces the frequency of $\mathrm{TM}_{1/2,0}$ mode and tunes it with respect to the frequency of TM_{10} mode, as given in Fig. 2(a). The gap-coupling between co-axially fed shorted microstrip line and rectangular patch results in a loop in the Smith chart. The horizontal length (l_h) of shorted microstrip line feed is smaller than the vertical length. It was noted in the parametric study that variation in this length primarily affects loop size and its position in the smith chart as represented in Fig. 2(b), and the frequency of $\mathrm{TM}_{1/2,0}$ mode. The variation in gap between the microstrip line and RMSA alters the mutual coupling between the two resonators and thus affects the input impedance at them as shown in Fig. 2(c). Thus, by optimizing the shorted microstrip line feed parameters, maximum S_{11} BW is obtained,

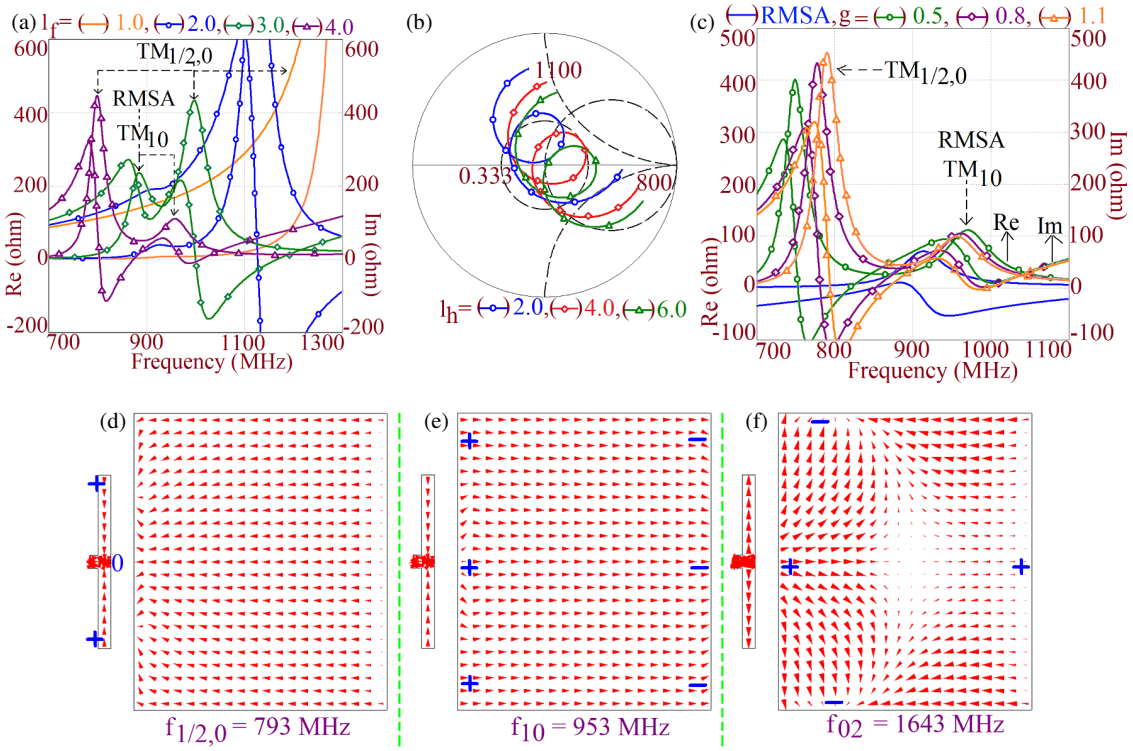

FIGURE 2. (a) Resonance plots for the variation in shorted microstrip line vertical length 'l_f', feeding the RMSA, (b) smith chart for variation in shorted microstrip line horizontal length, (c) resonance frequency plots for air gap variation between microstrip line and patch, and (d)–(f) peripheral current distribution at identified resonant modes for the design of shorted microstrip line feeding the RMSA .

and antenna parameters in the same are $L = 12$, $W = 14$, $h = 0.16$, $h_a = 1.0$, $l_f = 4.1$, $w_f = 0.6$, $l_h = 0.4$ cm. The simulated and experimental S_{11} BWs are 173 MHz (18.47%) and 171 MHz (18.3%), respectively as given in Fig. 3(a).

With a peak gain of more than 7 dBi, the MSA produces a broadside radiation pattern throughout the S_{11} BW. The E-plane of radiation is aligned along $\Phi = 0°$. The next resonant mode in rectangular patch is TM_{02} as shown in Fig. 2(f). The increment in BW is achieved by adjusting this frequency according to $TM_{1/2,0}$ mode of microstrip line and TM_{10} mode in RMSA. This is achieved by employing a pair of slots in RMSA, thus realizing the E-shape MSA as specified in Fig. 1(a). The optimization procedure for wideband E-shape MSA is well described in the literature [25] and hence not presented here. By optimizing a pair of slot parameters, wideband response in E-shape MSA is obtained, and results for them for slot parameters, as $l_s = 4.6$, $y_s = 1.95$, $w_s = 0.5$ cm, are shown in Fig. 3(a). Simulated and experimental S_{11} BWs are 198 MHz (20.93%) and 205 MHz (21.54%), respectively. The antenna accomplishes broadside radiation pattern across the S_{11} BW with the E-plane of radiation aligned along $\Phi = 0°$. The cross-polar level of radiation is lower by 15 dB as compared with the co-polar level of radiation. The maximum antenna gain is greater than 7 dBi. Thus, as compared with RMSA, E-shape design offers BW increment by 3%. To increase the BW further, additional resonators need to be added in the configuration. This can be realized by gap-coupling parasitic patches around the fed patch [27–29] or by embedding additional resonant slots inside the E-shape MSA. The addition of parasitic patches boosts the antenna size. While employing additional slots, variations in the impedance at different resonant modes inside the E-shape patch increase which does not yield impedance matching for the wideband response. Therefore, instead of these two methods, printed rectangular loop resonator was added outside the boundaries of E-shape MSA as displayed in Figs. 1(a), (b). The printed resonator loop lies below the E-shape MSA and hence does not increase the patch size. The coupling of electromagnetic energy from the patch to the loop excites the resonant mode to achieve an increment in the MSA BW. Resonance curve plots and surface current distribution for this extra mode excitation are displayed in Figs. 3(b)–(e) and 4(a), (b), which are the results of parametric analysis for the modification in printed resonator loop dimensions.

As recognized from the surface current distributions, first two modes correspond to $TM_{1/2,0}$ and TM_{10} mode in shorted microstrip line feed and rectangular patch, respectively. The third mode is due to the modified TM_0 mode as the surface currents are circulating around the slot length, thus, showing two half wavelength variation along slot cut RMSA width. At the fourth mode, currents exhibit two half wavelength variation along printed rectangular resonator length. With this distribution, this mode is referred to as TM_{20r}. In Fig. 3(e), back view of the configuration is shown so as to provide the surface current distribution on the rectangular loop. As the surface currents are circulating around horizontal and vertical lengths of rectangular loop, both the dimensions, L_c and L_1, affect its resonance frequency. The variations in them tune TM_{20r} mode frequency with reference to TM_{10}, TM_{02}, and $TM_{1/2,0}$ mode

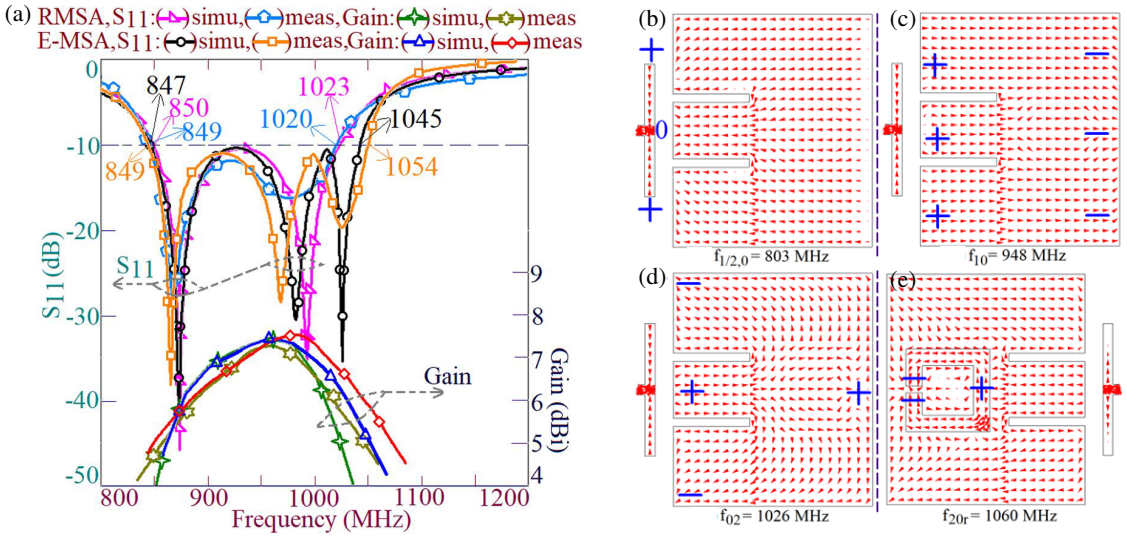

FIGURE 3. (a) S_{11} BW and gain plots, for shorted microstrip line fed RMSA and E-shape MSA, (b)–(e) peripheral surface current distribution at the observed resonant modes for microstrip line fed E-shape MSA loaded with printed rectangular loop resonator.

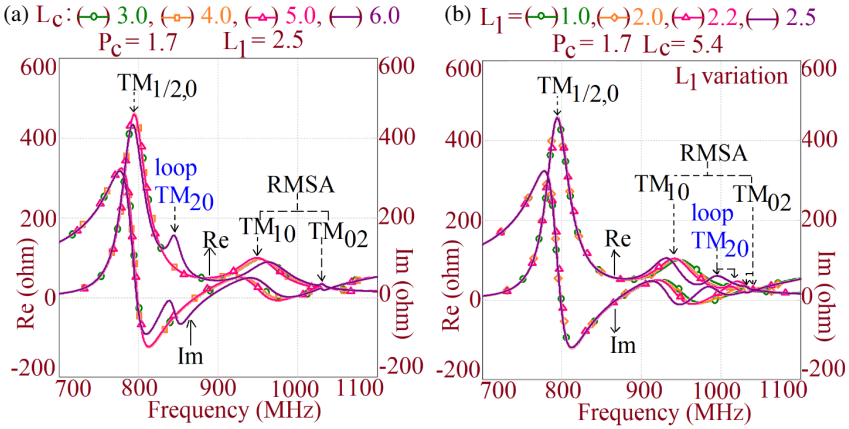

FIGURE 4. (a) (b) Resonance curve plots for the variation in printed rectangular resonator loop parameters for microstrip line fed E-shape MSA loaded with printed rectangular loop.

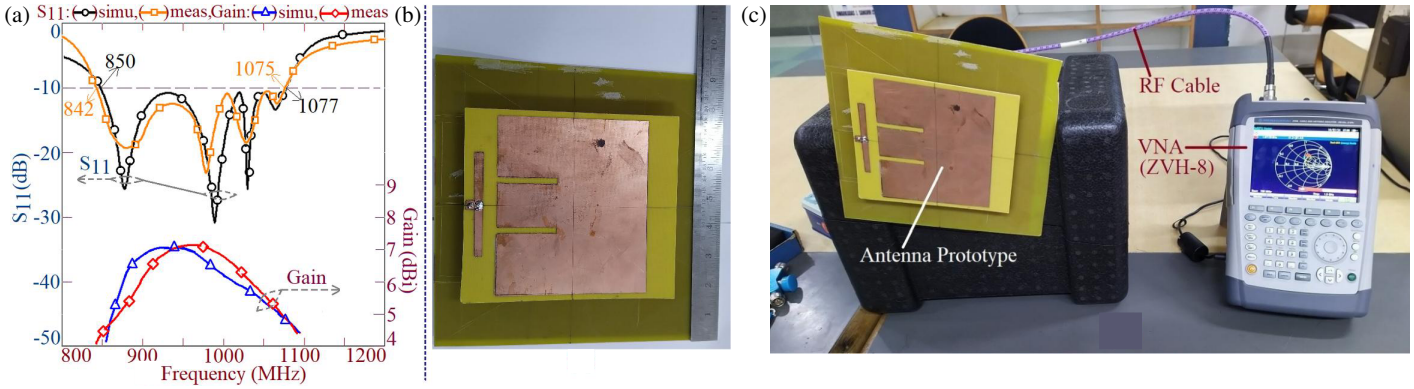

FIGURE 5. (a) S_{11} BW and gain plots, (b) fabricated antenna and (c) S_{11} BW measurement setup for microstrip line fed E-shape MSA loaded with printed rectangular resonator loop.

frequencies of shorted microstrip line and E-shape MSA. An optimum inter-spacing between them yields wider BW. While optimizing BW, another important design parameter is the position of the loop (P_c) with respect to E-shape MSA. For the orientation of the printed loop shown in Fig. 1(a), when the printed loop is placed below a pair of slots in E-shape MSA, the loop in

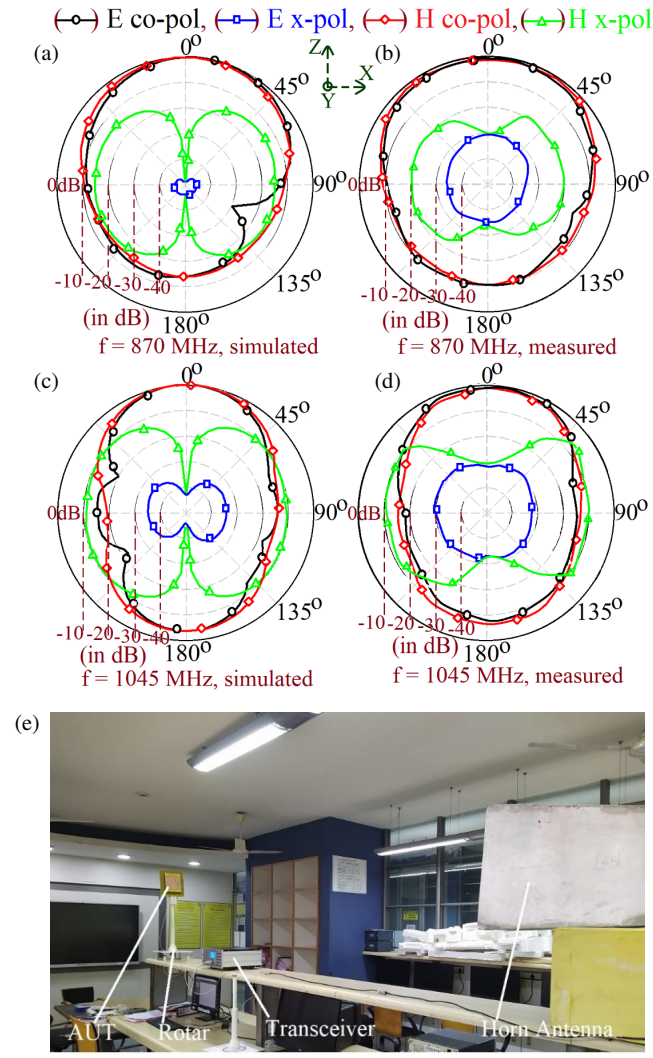

FIGURE 6. Radiation pattern near band (a) (b) start and (c) (d) stop frequencies of S_{11} BW, and (e) radiation pattern measurement setup for shorted microstrip line fed E-shape MSA loaded with printed rectangular resonator loop.

the Smith chart due to it or corresponding resonant peak in the resonance frequency plot is missing. For the loop position below the slots, maximum field point on the patch coincides with the minimum field point on the rectangular loop, because the coupling between them is poor, hence the loop is not observed. The coupling is present when the loop is placed on other side of the pair of slots, as maximum of resonant field points on loop and E-shape MSA coincides. Thus, while using this parametric study, wideband response in shorted microstrip line fed E-shape MSA loaded with printed rectangular loop resonator is obtained, and antenna parameters in the optimum design are $L = 12$, $W = 14$, $h = 0.16$, $h_a = 1.0$, $l_f = 4.1$, $w_f = 0.6$, $l_h = 0.4$, $l_s = 4.6$, $y_s = 1.95$, $w_s = 0.5$, $L_c = 5.1$, $L_1 = 2.25$, $w_c = 1.0$, $g_c = 0.4$ cm. For the ground plane dimensions as 20×20 cm, results for the optimum design are displayed in Figs. 5, 6, and 7(a). The antenna offers simulated and measured S_{11} BWs of 227 MHz (23.56%) and 233 MHz (24.3%), respectively. This is notably a higher value obtained on a thinner substrate. As the resonator rectangular loop is present beneath the patch, it is not visible in the fabricated antenna mentioned in Figs. 5(b), (c). The radiation pattern across the S_{11} BW is in the broadside direction with cross polar level below 15 dB in contrast to the co-polar level of radiation. The E-plane is along $\Phi = 0°$, over the complete BW. Antenna offers peak broadside gain of greater than 7 dBi.

The radiation pattern and gain measurements were conducted inside an antenna laboratory. In the measurements, wideband and high gain Horn antenna was used as the reference. A far-field distance is calculated with respect to the higher frequency of S_{11} BW, and it is maintained between two antennas. The three-antenna method is used for broadside gain measurement. Another feature of microstrip line feed is the harmonic suppression. The simulated S_{11} plots for microstrip line fed E-shape MSA with a rectangular loop against the coaxially fed E-shape MSA are provided in Fig. 7(b). As noted in Fig. 7(b), the selection of shorted feed line provides a suppression in the higher frequency components.

3. DESIGN METHODOLOGY FOR SHORTED MICROSTRIP LINE FED E-SHAPE MSA LOADED WITH RECTANGULAR LOOP RESONATOR

An optimum BW in shorted microstrip line fed E-shape MSA loaded with a rectangular resonator loop is because of the optimum spacing among the $\mathrm{TM}_{1/2,0}$ mode of shorted line, TM_{10} and TM_{02} modes of rectangular patch, and TM_{20r} mode on printed rectangular loop resonator. In this section, initially the resonant length formulation at each of these modes is proposed. To derive each of the formulation, peripheral current distribution at each mode is analyzed based on which, formulation is realized. Peripheral currents at $\mathrm{TM}_{1/2,0}$ mode vary by a quarter wavelength along the shorted length, and Equation (1) provides the resonant length at the same. Equation (2) is used to find the frequency. For the shorted line parameters as $h = 0.16$, $h_a = 1.0$, $l_f = 4.1$, $w_f = 0.6$, $l_h = 0.4$ cm, frequency calculated using (2) is 812 MHz that agrees closely with the simulated frequency of 804 MHz. The configuration of the microstrip line-fed E-shape MSA paired with the rectangular loop resonator shows this simulated frequency. The equations mentioned in this section provide frequency in GHz and antenna size in cm.

$$L_{e120} = l_f + 2\,(1.85 h_t) \tag{1}$$

$$f_{120} = 30/4L_{e120}\sqrt{\varepsilon_{re}} \tag{2}$$

The resonant length at TM_{10} mode in E-shape MSA is formulated with Equation (3). In E-shape patch, a pair of rectangular slots are parallel to the TM_{10} modal currents, and thus TM_{10} mode frequency of equivalent RMSA marginally differs from the TM_{10} mode frequency observed in E-shape MSA [25]. The frequency is calculated using Equation (4). The effective dielectric constant (ε_{re}) in three-layer air suspended configuration is computed using Equation (5). For the antenna dimensions as $L = 12$, $W = 14$, $h = 0.16$, $h_a = 1.0$ cm and using FR4 substrate, calculated frequency is 956 MHz, which

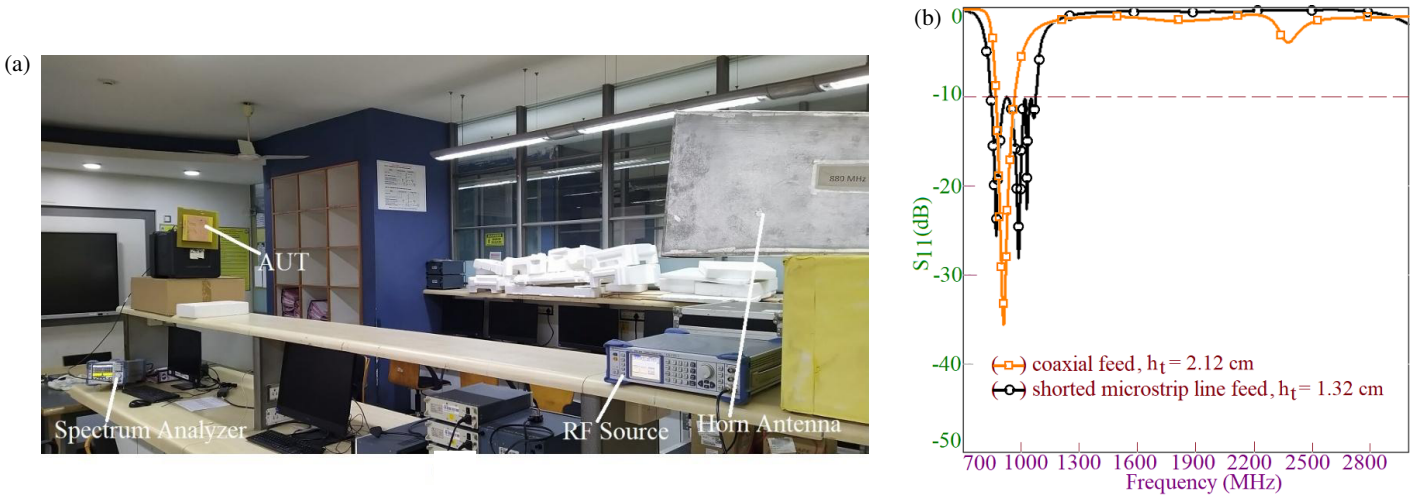

FIGURE 7. (a) Broadside gain measurement setup for microstrip line fed E-shape MSA loaded with printed rectangular resonator loop, (b) S_{11} BW plots for coaxially fed E-shape MSA against shorted microstrip line fed E-shape MSA coupled with printed rectangular loop.

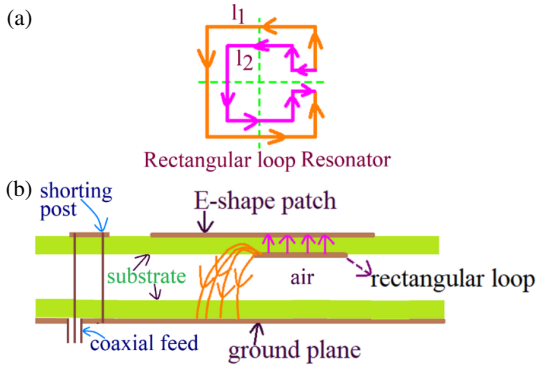

FIGURE 8. (a) Resonant length path for rectangular loop resonant mode and (b) fringing fields for printed rectangular loop resonator.

matches closely with simulated frequency of 946 MHz.

$$L_{e10} = L + 2\,(0.9h_t) \tag{3}$$

$$f_{10} = 30/2L_{e10}\sqrt{\varepsilon_{re}} \tag{4}$$

$$\varepsilon_{re} = \frac{\varepsilon_r^2\,(2h+h_a)}{2h\varepsilon_r+h_a\varepsilon_r^2} \tag{5}$$

In E-shape patch, a pair of rectangular slots perturb the peripheral current directions at TM_{02} mode. The effective patch width of TM_{02} mode is calculated using Equation (6), and the frequency is calculated with Equation (7). The frequency calculated using (7) is 1034 MHz, which is quite close to the 1025 MHz simulated frequency.

$$W_{e02} = W + 2\,(1.3h_t) + 4l_s\,(1.3l_s/L) \tag{6}$$

$$f_{02es} = 30/W_{e02}\sqrt{\varepsilon_{re}} \tag{7}$$

Surface currents in the rectangular resonator loop exhibit two half wavelength variation across the whole loop length at TM_{20r} mode. In this effective resonant length (l_{20r}) is realized by taking average of two lengths, l_1 and l_2, as shown in Fig. 8(a) and provided in Equation (8). The frequency is determined using Equation (9). The ε_{re} for the rectangular loop mode is calculated using Equation (10).

$$l_{20r} = 2L_c+4L_1+g_c-3w_c \tag{8}$$

$$f_{02es} = 30/W_{e02}\sqrt{\varepsilon_{re}} \tag{9}$$

$$\varepsilon_{r1} = \varepsilon_r+\varepsilon_{re}/2 \tag{10}$$

One side of the rectangular loop has a ground plane with an air dielectric, while the other side has an FR4 substrate with an E-shaped patch. The fringing fields arising from rectangular loop resides between the loop and E-shape MSA, which sees effective dielectric constant as that of substrate. However, as Fig. 8(b) illustrates, there is an equal contribution of fringing fields that either go through the substrate and then through the air and substrate to the ground plane, or they pass through the air and ground plane. With this air-substrate-air interface, the later part sees effective permittivity as that of suspended dielectric in the air in the three-layer configuration. Therefore, rectangular loop sees two effective dielectric constants on the two sides. Therefore, the average value of two dielectric constants is considered for the effective dielectric constant calculation as mentioned in Equation (10). For the antenna dimensions present in the optimum configuration, computed modal frequency of TM_{20r} is 1054 MHz, which is close to the simulated frequency of 1060 MHz.

Using the proposed formulation, the methodology to design shorted microstrip line fed E-shape MSA loaded with printed rectangular loop is presented. The design begins with a mention of band start frequency of the BW 'f_{st}'. In the design methodology, above resonant length formulations and various resonant mode frequency and patch dimension relations present in the above optimum design have been utilized. The TM_{10} mode frequency of E-shape MSA is computed using (11). The total substrate thickness is evaluated using Equations (12) and (13). As the design employs three-layer suspended configuration, the total substrate thickness involves air gap thickness and FR4 substrate thickness. Since the air gap thickness is unknown to begin with, the value of ε_{re} is not available. Since the total substrate thickness mentioned in (13) is the same as the sub-

strate thickness used in the above optimum design, ε_{re} is taken as 1.223. From the calculated value of h_t, the value of h_a is selected that is an integer number or practically realizable value. Using it and for FR4 substrate, ε_{re} and operating wavelength at TM_{10} mode are recalculated by using Equations (5) and (12), respectively. The patch length and width in E-shape patch are calculated using Equations (14) and (15).

$$f_{10} = 1.113 f_{st} \quad (11)$$

$$\lambda_{g10} = 30/f_{10}\sqrt{\varepsilon_{re}} \quad (12)$$

$$h_t = 0.046\lambda_{g10} \quad (13)$$

$$L = (30/2f_{10}\sqrt{\varepsilon_{re}}) - 1.8h_t \quad (14)$$

$$W = 1.1667L \quad (15)$$

The $TM_{1/2,0}$ mode frequency of the shorted microstrip line bears a frequency relation $f_{120} = 0.946 f_{st}$ with respect to band start frequency of BW. Using this and Equations (16) and (17), shorted microstrip line width l_f is calculated. The width of microstrip line w_f and its horizontal length l_h are calculated as $0.15l_f$ and $0.1l_f$, respectively.

$$l_{sf} = 30/4f_{120}\sqrt{\varepsilon_{re}} \quad (16)$$

$$l_f = l_{sf} - 2\,(1.85h_t) \quad (17)$$

The modified TM_{02} mode frequency in the microstrip line fed design of E-shape MSA bears a frequency relation $f_{02e} = 1.206 f_{st}$, with respect to the band start frequency of BW. Using this and Equation (18), modified patch width (W_{es02}) that includes the effects of a pair of slots is calculated. Further, using Equation (19), slot length 'l_s' is obtained. This equation is realized by rearranging the terms on two sides of the Equation (6). The separation between the pair of slots (y_s) and slot width (w_s) are calculated as $0.4243l_s$ and $0.1087l_s$, respectively.

$$W_{es02} = 30/f_{02e}\sqrt{\varepsilon_{re}} \quad (18)$$

$$l_s = \sqrt{L\,(W_{es02} - W - 2.6h_t)\,/5.2} \quad (19)$$

The TM_{20r} mode frequency on the printed rectangular loop bears a frequency relation $f_{20r} = 1.2435 f_{st}$ with respect to the band start frequency of the BW. Using this and Equation (20), effective resonant length (l_{r20}) is determined. The ε_{re} mentioned in Equation (20) is the average of ε_{re} for three layer suspended dielectric substrate and the dielectric constant of FR4 substrate, as mentioned in Equation (10). For the effective resonant length mentioned in (8), printed loop dimensions like L_c, L_1, g_c and w_c are present. To simplify the calculation, relations between various loop dimensions as $L_c = 2.266L_1$, $g_c = 0.1778L_1$ and $w_c = 0.444L_1$ are used. Using this, Equation (8) is simplified, and further terms on the two sides of the same are rearranged to evaluate loop dimension L_1, as mentioned in Equation (21). Using above relations, all other printed loop dimensions are calculated. The center of the loop is placed at distance $P_c = 0.192L$, on other side of the pair of slots and below the patch. Lastly, an air gap between the shorted microstrip line feed and E-shape MSA (g) is maintained equal to $0.833h_t$.

$$l_{r20} = 30/f_{20r}\sqrt{\varepsilon_{r1}} \quad (20)$$

$$L_1 = l_{r20}/7.3768 \quad (21)$$

Using the above design methodology, shorted microstrip line fed E-shape MSA loaded with a printed rectangular loop is designed for $f_{st} = 1000$ MHz, and various antenna parameters for this design calculated using above procedure are $L = 9.9$, $W = 11.5$, $h = 0.16$, $h_a = 0.8$, $l_f = 2.95$, $w_f = 0.4$, $l_h = 0.3$, $l_s = 3.8$, $y_s = 1.6$, $w_s = 0.4$, $L_c = 4.4$, $L_1 = 2.0$, $w_c = 0.9$, $g_c = 0.3$, $g = 0.9$ cm. The antenna S_{11} BWs observed in the simulation and measurement is 283 MHz (24.32%) and 291 MHz (24.86%), respectively. The antenna offers broadside peak gain larger than 7.0 dBi. The start frequency of S_{11} BW in the simulation is found to be 1022 MHz, which is close to the desired frequency selected. This validates the design methodology. Using the above design methodology, for some of the antenna parameters, non-integer values are obtained. While they are designed practically, those values are rounded off to the nearest integer or practically realizable value. Due to this, the variation in expected results is observed. Therefore, in some of the redesigned configuration, minor parametric optimization is needed to arrive at the final optimum configuration. Thus, using the proposed design methodology, wideband E-shape MSA on a thinner substrate can be designed around the specific band start frequency of S_{11} BW, which can be as per given wireless application.

4. RESULTS AND COMPARATIVE ANALYSIS

The design of microstrip line fed E-shape MSA loaded with printed rectangular loop resonator offers maximum BW and gain amongst the proposed designs. Therefore, to present the novelty in the present study, its comparison to the reported wideband configurations, realized using multi-resonator gap-coupled stacked designs, modified shapes of the radiating patch, resonant slot cut antennas or modified ground plane configuration, is presented in Table 1. The comparative study is presented on points namely, measured S_{11} BW and peak gain, against antenna volume, i.e., patch size and substrate thickness. The reported designs are optimized in different frequency bands and substrate thickness. Thus, to compare them against the proposed design, antenna patch area and substrate thickness are normalized with respect to the wavelength (λ_c) at the center frequency of S_{11} BW.

The wideband gap-coupled design discussed in [5] offers much larger gain, but patch size is larger due to the offset patches present in the design. The gap-coupled sector and arc shape design discussed in [6] offers lower gain. The wideband design presented in [7] employs multiple parasitic shorted patches, whereas gap-coupled configuration presented in [8] in 15000 MHz frequency band, requires a thicker substrate. The multi-resonator design discussed in [9, 10] offers higher gain and BW, but it uses patches in gap-coupled and stacked layer and also employs a cavity-backed configuration. Due to this antenna thickness is more. The wideband designs discussed in [11, 12] employ shorted microstrip line feeding. The antenna discussed in [11] offers equivalent antenna gain on a similar substrate thickness to the proposed design. But the proposed design offers higher BW. Also, in [11, 12], details about resonant mode excited in shorted microstrip line feeding and design guidelines for the wideband antenna are not provided.

TABLE 1. Comparison for proposed wideband MSA against reported MSAs.

MSA shown in	Measured BW (MHz, %)	Peak Gain (dBi)	Area(A_P/λ_c^2)	Substrate thickness (h_t/λ_c)
Fig. 1	233, 24.3	7.1	0.241	0.046
Ref. [5]	1200, 12.3	12	7.595	0.105
Ref. [6]	—, 6.3	<0 dBi	2.22	0.068
Ref. [7]	810, 13.8	5.0	0.973	0.067
Ref. [8]	6300, 40	10	1.027	0.113
Ref. [9]	1680, 64.12	12.45	0.356	0.105
Ref. [10]	1114, 55.7	12.3	1.073	0.155
Ref. [11]	660, 11.5	7.07	1.491	0.042
Ref. [12]	21, 1	< 0 dBi	0.3435	0.018
Ref. [13]	350, 6.8	7.0	0.201	0.04
Ref. [14]	600, 6.1	7.0	0.632	0.02
Ref. [15]	470, 44.9	10	0.343	0.08
Ref. [16]	408, 24.82	7.2	0.209	0.076
Ref. [17]	3000, 53.6	10.2	0.429	0.124
Ref. [18]	3100, 12	6.8	> 6	0.144
Ref. [19]	2040, 68	10	0.33	0.023
Ref. [20]	7700, 110	4.5	0.533	0.06
Ref. [21]	1960, 30.1	8.0	0.855	0.054
Ref. [22]	168, 12.88	1.8	0.42	0.013
Ref. [23]	351, 39.1	6.0	0.143	0.065
Ref. [24]	240, 26.4	6.0	0.14	0.042
Ref. [27]	1500, 27.3	6.4	0.456	0.061
Ref. [28]	1440, 26.2	8.5	0.811	0.115
Ref. [29]	835, 58.12	8.8	0.234	0.125
Ref. [31]	969, 69.84	9	0.322	0.13
Ref. [32]	130, 13.89	7.6	0.225	0.039

A thinner substrate modified patch shape designs discussed in [13, 14] does offer equivalent antenna gain, but they have lower S_{11} BW than the proposed design. The initial reported wideband designs employing U-slot or a pair of rectangular slots [15, 16] offer higher BW than the proposed configuration. However, antenna volume is higher. The multiple slots cut antenna discussed in [17] requires a thicker substrate. The double U-slot cut antenna discussed in [18] requires larger antenna volume, whereas thinner substrate double U-slot cut wideband rectangular patch presented in [19] employs differential feeding. The wideband designs discussed in [20, 21] employ multiple patches as well as modified ground plane structure. They do offer higher BW, but for the work reported, details about antenna functioning in terms resonant modes of the antenna cavity are not presented. Also, the overall design is complex against the proposed configuration. The bow-tie shape ground plane designs discussed in [22–24] offer lower peak and average gain, due to the unwanted radiation taking place in the back-lobe. The wideband designs discussed in [27–29] employ parasitic patches around the fed patch. With this they offer higher BW but require thicker antenna substrate. For the multi-resonator design presented in [27], antenna gain is lower than the proposed configuration. The wideband E-shape design discussed in [31] requires higher patch size as it employs parasitic C-shape patches. Also it is optimized on a thicker substrate against the proposed thinner substrate microstrip line fed MSA. The wideband E-shape MSA discussed in [32], on nearly the same substrate thickness and patch area, has 10% lower S_{11} BW than the proposed design. This is due to the use of shorted microstrip line feed in the proposed design compared to the coaxial feed employed in [32].

In the reported wideband slot cut antennas offering broadside radiation characteristics, a thicker substrate is needed. Against this, the proposed design employs shorted microstrip line feeding that helps in achieving the wideband response in E-shape patch on a thinner substrate ($< 0.05\lambda_g$). Increment in the BW of E-shape patch is further achieved by employing a printed rectangular loop resonator as parasitic element that is kept below the patch. This parasitic patch arrangement ensures no further increase in the antenna size. Also, the microstrip line feeding provides harmonic frequency suppression at higher frequencies as shown from the S_{11} plots. The modified ground plane profile is not employed in the proposed configuration, thus limiting the decrement in gain arising from the back-lobe radiation. Thus, the proposed work does not just put forward another wideband E-shape design, but presents a systematic

study that helps in reducing the substrate thickness and achieves wider BW without using additional coupled resonators. Also in the tabular comparison above, it is shown that how proposed work shows improvement in the results compared to earlier reported wideband E-shape MSA on thicker and thinner substrates. Therefore, a wideband design of slot cut MSA while employing microstrip line feeding on thinner substrate is the new technical contribution in the proposed work.

5. CONCLUSIONS

Wideband design of shorted microstrip line fed E-shape MSA loaded with a printed rectangular loop resonator is presented on electrically thinner substrate. In 900 MHz frequency spectrum, MSA provides a BW of 24% with a peak broadside gain of more than 7 dBi on substrate thickness of $0.046\lambda_g$. Compared to the reported designs, proposed configurations provide improved BW and gain results, on a thinner substrate while offering broadside radiation characteristics. The use of microstrip line feed also achieves harmonic suppression in the higher frequency band. The design methodology is proposed for thinner substrate slot cut antenna that helps in designing a similar configuration in different frequency bands as per specific wireless application.

REFERENCES

[1] Kumar, G. and K. P. Ray, *Broadband Microstrip Antennas*, Artech House, 2003.

[2] Garg, R., *Microstrip Antenna Design Handbook*, Artech House, 2001.

[3] Balanis, C. A., *Antenna Theory: Analysis and Design*, 2nd ed., John Wiley & Sons, USA, 2007.

[4] Kovitz, J. M. and Y. Rahmat-Samii, "Using thick substrates and capacitive probe compensation to enhance the bandwidth of traditional CP patch antennas," *IEEE Transactions on Antennas and Propagation*, Vol. 62, No. 10, 4970–4979, Oct. 2014.

[5] Kandwal, A. and S. K. Khah, "A novel design of gap-coupled sectoral patch antenna," *IEEE Antennas and Wireless Propagation Letters*, Vol. 12, 674–677, 2013.

[6] Balaji, U., "Bandwidth enhanced circular and annular ring sectoral patch antennas," *Progress In Electromagnetics Research Letters*, Vol. 84, 67–73, 2019.

[7] Xu, K. D., H. Xu, Y. Liu, J. Li, and Q. H. Liu, "Microstrip patch antennas with multiple parasitic patches and shorting vias for bandwidth enhancement," *IEEE Access*, Vol. 6, 11 624–11 633, 2018.

[8] Cao, Y., Y. Cai, W. Cao, B. Xi, Z. Qian, T. Wu, and L. Zhu, "Broadband and high-gain microstrip patch antenna loaded with parasitic mushroom-type structure," *IEEE Antennas and Wireless Propagation Letters*, Vol. 18, No. 7, 1405–1409, Jul. 2019.

[9] Raha, K. and K. P. Ray, "Broadband high gain and low cross-polarization double cavity-backed stacked microstrip antenna," *IEEE Transactions on Antennas and Propagation*, Vol. 70, No. 7, 5902–5906, Jul. 2022.

[10] Chopra, R. and G. Kumar, "Broadband and high gain multilayer multiresonator elliptical microstrip antenna," *IET Microwaves, Antennas & Propagation*, Vol. 14, No. 8, 821–829, 2020.

[11] Rathod, S. M., R. N. Awale, K. P. Ray, and A. D. Chaudhari, "Broadband gap-coupled half-hexagonal microstrip antenna fed by microstrip-line resonator," *International Journal of RF and Microwave Computer-Aided Engineering*, Vol. 28, No. 6, e21273, 2018.

[12] Rathod, S. M., R. N. Awale, and K. P. Ray, "A 50ω microstrip line fed shorted hexagonal microstrip antennas with reduced cross-polarization," *Journal of Microwaves, Optoelectronics and Electromagnetic Applications*, Vol. 18, No. 2, 246–262, 2019.

[13] Yoo, J.-U. and H.-W. Son, "A simple compact wideband microstrip antenna consisting of three staggered patches," *IEEE Antennas and Wireless Propagation Letters*, Vol. 19, No. 12, 2038–2042, 2020.

[14] Muntoni, G., G. Montisci, G. A. Casula, F. P. Chietera, A. Michel, R. Colella, L. Catarinucci, and G. Mazzarella, "A curved 3-D printed microstrip patch antenna layout for bandwidth enhancement and size reduction," *IEEE Antennas and Wireless Propagation Letters*, Vol. 19, No. 7, 1118–1122, Jul. 2020.

[15] Huynh, T. and K.-F. Lee, "Single-layer single-patch wideband microstrip antenna," *Electronics Letters*, Vol. 31, No. 16, 1310–1312, Aug. 1995.

[16] Wong, K.-L. and W.-H. Hsu, "A broad-band rectangular patch antenna with a pair of wide slits," *IEEE Transactions on Antennas and Propagation*, Vol. 49, No. 9, 1345–1347, Sep. 2001.

[17] Sharma, S. K. and L. Shafai, "Performance of a novel ψ-shape microstrip patch antenna with wide bandwidth," *IEEE Antennas and Wireless Propagation Letters*, Vol. 8, 468–471, 2009.

[18] Fan, T.-Q., B. Jiang, R. Liu, J. Xiu, Y. Lin, and H. Xu, "A novel double U-slot microstrip patch antenna design for low-profile and broad bandwidth applications," *IEEE Transactions on Antennas and Propagation*, Vol. 70, No. 4, 2543–2549, 2022.

[19] Radavaram, S. and M. Pour, "Wideband radiation reconfigurable microstrip patch antenna loaded with two inverted U-slots," *IEEE Transactions on Antennas and Propagation*, Vol. 67, No. 3, 1501–1508, Mar. 2019.

[20] Baudha, S. and M. V. Yadav, "A novel design of a planar antenna with modified patch and defective ground plane for ultra-wideband applications," *Microwave and Optical Technology Letters*, Vol. 61, No. 5, 1320–1327, 2019.

[21] Mondal, K. and P. P. Sarkar, "Gain and bandwidth enhancement of microstrip patch antenna for WiMAX and WLAN applications," *IETE Journal of Research*, Vol. 67, No. 5, 726–734, 2021.

[22] Kadam, P. A. and A. A. Deshmukh, "Designs of regular shape microstrip antennas backed by bow-tie shape ground plane for enhanced antenna characteristics," *AEU — International Journal of Electronics and Communications*, Vol. 137, 153823, 2021.

[23] Chavali, V. A. P. and A. A. Deshmukh, "Wideband designs of regular shape microstrip antennas using modified ground plane," *Progress In Electromagnetics Research C*, Vol. 117, 203–219, 2021.

[24] Deshmukh, A. A., V. A. P. Chavali, and A. G. Ambekar, "Thinner substrate designs of modified ground plane E-shape microstrip antennas for wideband response," *Electromagnetics*, Vol. 42, No. 4, 255–265, 2022.

[25] Deshmukh, A. A. and K. P. Ray, "Analysis of broadband Psi (Ψ)-shaped microstrip antennas," *IEEE Antennas and Propagation Magazine*, Vol. 55, No. 2, 107–123, 2013.

[26] "Cst software," Version 2019.

[27] Wi, S.-H., Y.-S. Lee, and J.-G. Yook, "Wideband microstrip patch antenna with U-shaped parasitic elements," *IEEE Transactions on Antennas and Propagation*, Vol. 55, No. 4, 1196–1199, 2007.

[28] Lu, H.-X., F. Liu, M. Su, and Y.-A. Liu, "Design and analysis of wideband U-slot patch antenna with U-shaped parasitic elements," *International Journal of RF and Microwave Computer-*

Aided Engineering, Vol. 28, No. 2, e21202, 2018.

[29] Chavali, V. A. P. and A. A. Deshmukh, "Wideband designs of proximity fed isosceles triangular microstrip antennas gap-coupled with parasitic pairs of sectoral patches," *International Journal of RF and Microwave Computer-Aided Engineering*, Vol. 32, No. 6, e23132, 2022.

[30] Liu, N.-W., L. Zhu, W.-W. Choi, and X. Zhang, "Wideband shorted patch antenna under radiation of dual-resonant modes," *IEEE Transactions on Antennas and Propagation*, Vol. 65, No. 6, 2789–2796, 2017.

[31] Chavali, V. A. P. and A. A. Deshmukh, "Multi resonant gap-coupled designs of E-shape microstrip antenna for wideband response," *Progress In Electromagnetics Research C*, Vol. 149, 67–79, 2024.

[32] Chavali, V. A. P. and A. A. Deshmukh, "Wideband designs of E-shape microstrip antenna on thinner substrate," *Journal of Microwaves, Optoelectronics and Electromagnetic Applications*, Vol. 24, No. 2, e2024291826, 2025.